THE JOURNAL OF BIOLOGICAL CHEMISTRY
Vol. 278, No. 43, Issue of October 24, pp. 42283–42293, 2003
Printed in U.S.A.
© 2003 by The American Society for Biochemistry and Molecular Biology, Inc.

The Specific Interaction of Dinitrosyl-Diglutathionyl-Iron Complex, a Natural NO Carrier, with the Glutathione Transferase Superfamily

SUGGESTION FOR AN EVOLUTIONARY PRESSURE IN THE DIRECTION OF THE STORAGE OF NITRIC OXIDE*

Received for publication, May 28, 2003, and in revised form, July 10, 2003
Published, JBC Papers in Press, July 18, 2003, DOI 10.1074/jbc.M305568200

Francesca De Maria‡, Jens Z. Pedersen§, Anna Maria Caccuri‡¶‖, Giovanni Antonini‖, Paola Turella‡, Lorenzo Stella‡, Mario Lo Bello§¶, Giorgio Federici‡‡, and Giorgio Ricci‡¶‖‡‡§§**

*From the ‡Department of Chemical Sciences and Technologies and §Department of Biology, University of Rome "Tor Vergata," 00133 Rome, the **Department of Biology, University of Rome "Roma Tre," 00146 Rome, and ‡‡Children's Hospital IRCCS "Bambin Gesù," 00165 Rome, Italy*

The interaction of dinitrosyl-diglutathionyl-iron complex (DNDGIC), a natural carrier of nitric oxide, with representative members of the human glutathione transferase (GST) superfamily, *i.e.* GSTA1-1, GSTM2-2, GSTP1-1, and GSTT2-2, has been investigated by means of pre-steady and steady state kinetics, fluorometry, electron paramagnetic resonance, and radiometric experiments. This complex binds with extraordinary affinity to the active site of all these dimeric enzymes; GSTA1-1 shows the strongest interaction ($K_D \cong 10^{-10}$ M), whereas GSTM2-2 and GSTP1-1 display similar and slightly lower affinities ($K_D \cong 10^{-9}$ M). Binding of the complex to GSTA1-1 triggers structural intersubunit communication, which lowers the affinity for DNDGIC in the vacant subunit and also causes a drastic loss of enzyme activity. Negative cooperativity is also found in GSTM2-2 and GSTP1-1, but it does not affect the catalytic competence of the second subunit. Stopped-flow and fluorescence data fit well to a common minimal binding mechanism, which includes an initial interaction with GSH and a slower bimolecular interaction of DNDGIC with one high and one low affinity binding site. Interestingly, the Theta class GSTT2-2, close to the ancestral precursor of GSTs, shows very slow binding kinetics and hundred times lowered affinity ($K_D \cong 10^{-7}$ M), whereas the bacterial GSTB1-1 is not inhibited by DNDGIC. Molecular modeling and EPR data reveal structural details that may explain the observed kinetic data. The optimized interaction with this NO carrier, developed in the more recently evolved GSTs, may be related to the acquired capacity to utilize NO as a signal messenger.

Glutathione *S*-transferases (GSTs)[1] (EC 2.5.1.18) are a superfamily of multifunctional enzymes able to protect the cell against endogenous or exogenous toxic compounds (1). The human cytosolic GSTs are homo- or heterodimeric proteins, encoded by distantly related gene families and grouped into eight classes termed Alpha, Kappa, Mu, Omega, Pi, Sigma, Theta, and Zeta (2–8) on the basis of sequence similarity, substrate and inhibitor specificity, immunological properties, and three-dimensional structure. The most important reaction catalyzed by GSTs is the conjugation of the sulfur atom of GSH to an electrophilic center of many toxic organic compounds. The Alpha class also shows an additional selenium-independent peroxidase activity with organic peroxides (9). Other physiological roles of GSTs include chemical sequestration (10), regulation of the Jun kinase protein (11), inhibition of the proapoptotic action of Bax (12), and modulation of calcium channels which oppose the apoptotic mobilization of calcium ions (13). In the last 10 years, the x-ray structures of representative members of the GST superfamily have been solved, showing similar three-dimensional folding of these proteins and very similar topography of the GSH-binding sites (G-sites) (14–17). Recently, we described the peculiar interaction between GSTP1-1 and dinitrosyl-diglutathionyl-iron complex (DNDGIC) (Scheme 1), a natural nitric oxide carrier that binds to the G-site with thousand times higher affinity than GSH (18). DNDGIC, which can be formed *in vivo* by free NO or NO donors, GSH, and traces of ferrous ion, is a paramagnetic molecule with a diagnostic electron paramagnetic resonance (EPR) spectrum centered at about $g = 2.03$ both in the frozen state at 77 and at 298 K (19). The occurrence of dinitrosyl-iron complexes (DNICs) in mammalian tissues and cells was observed more than 30 years ago after exposure of tissues to endogenous or exogenous NO (19). *In vivo*, DNDGIC and other low mass DNICs could be in equilibrium with several protein-bound forms after replacing one or both the free thiol ligands with protein residues like His, Cys and Ser (19). Both low mass and high mass DNICs seem to be more stable than NO and may possibly act as storage of nitric oxide (20–22) as well as intermediates in the iron-catalyzed formation and decomposition of *S*-nitrosothiols (23). DNICs also inhibit platelet aggregation (24), reduce blood pressure (25), relax vascular vessels (26), induce accumulation of heat shock protein HSP70 (27, 28), and modulate ion channel activity (29). The recently discovered interaction of DNDGIC with GSTP1-1 is of particular interest as this complex possibly represents the most potent natural competitive inhibitor of this enzyme (18). A particular intersubunit communication triggered by DNDGIC was also found, which lowers the affinity of the adjacent subunit. EPR spectroscopy and molecular modeling indicated that DNDGIC is stabilized in the G-site through the usual polar and hydrophobic interactions of protein resi-

* The costs of publication of this article were defrayed in part by the payment of page charges. This article must therefore be hereby marked "*advertisement*" in accordance with 18 U.S.C. Section 1734 solely to indicate this fact.
¶ Supported in part by MURST PRIN2002.
‖ Supported in part by National Research Council of Italy (Target Project on Biotechnology).
§§ To whom correspondence should be addressed: Dept. of Chemical Sciences and Technologies, University of Rome "Tor Vergata," Via della Ricerca Scientifica, 00133 Rome, Italy. Tel.: 39 0672594379; Fax: 39 0672594311; E-mail: riccig@uniroma2.it.
[1] The abbreviations used are: GST, glutathione *S*-transferase; CDNB, 1-chloro-2,4-dinitrobenzene; NBD-Cl, 7-chloro-4-nitrobenzo-2-oxa-1,3-diazole; Msu, menaphthyl sulfate; DNDGIC, dinitrosyl-diglutathionyl-iron complex; DNICs, dinitrosyl-iron complexes.

Downloaded from http://www.jbc.org/ by guest on July 18, 2018

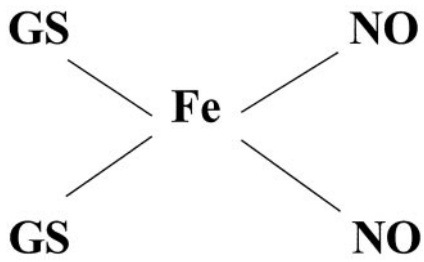

SCHEME 1

dues with one GSH molecule, coordination of the iron ion to the hydroxyl group of Tyr-7, and additional van der Waals interactions of NO moieties with Ile-104 and Tyr-108 (18). This interaction is quite surprising as it is a common opinion that the G-site recognizes GSH (and a few GSH analogs) almost exclusively. In addition, cooperative intersubunit communication in GSTP1-1 has only been observed after a few selected point mutations (30, 31) or under thermal stress (32) but never in the native enzyme under physiological conditions. The tight interaction between GSTP1-1 and an endogenous NO carrier is also indicative of an additional physiological role for this enzyme as an NO-storage protein. The surprising results of this paper demonstrate that not only GSTP1-1 but all representative members of mammalian GSTs interact with DNDGIC showing similar binding mechanism and cooperativity.

EXPERIMENTAL PROCEDURES

Enzyme Expression and Purification—Human GSTA1-1, GSTM2-2, and GSTP1-1 were expressed in *Escherichia coli* and purified as described previously (18, 33, 34). Expression of the human GSTT2-2 and its purification using immobilized metal ion chromatography on a nickel-nitrilotriacetic acid matrix (Qiagen, Hilden, Germany) were carried out as reported previously (35, 36). Expression and purification of the bacterial GSTB1-1 was performed as described in Ref. 37. The enzyme concentrations reported in the text for all GSTs refer to the single subunit.

DNDGIC Synthesis—DNDGIC was prepared essentially as described previously (18). Briefly, 1 ml of 0.5 mM $FeSO_4$ (dissolved in degassed water to avoid rapid oxidation to the ferric state) was added to 10 ml (final volume) of 0.1 M of potassium phosphate buffer, pH 7.4, containing 20 mM GSH and 2 mM GSNO (25 °C). After 10 min, the reaction was almost complete, and the resulting stock solution of DNDGIC (50 μM) was stable for at least 3 h. For the sake of simplicity, we have used the abbreviation DNDGIC also for the complex bound to GSTs, although the latter is shown to be a monoglutathionyl species.

Inhibition Experiments—Inhibition of GSTA1-1, GSTP1-1, and GSTM2-2 by DNDGIC was studied by incubating variable amounts of DNDGIC (from 0.4 to 9 μM) with a fixed enzyme concentration (4 μM) in 1 ml of 0.1 M potassium phosphate buffer, pH 7.4 (25 °C). After 2 min, 4-μl aliquots were diluted in 1 ml of 0.1 M potassium phosphate buffer, pH 6.5, containing 10 mM GSH and 1 mM 1-chloro-2,4-dinitrobenzene (CDNB). The enzyme activity was determined spectrophotometrically at 340 nm (25 °C) (ϵ = 9,600 M^{-1} cm^{-1} for the DNB-GSH adduct) within 10 s from addition of the substrates. This procedure, mentioned in the text as "assay under non-equilibrium conditions" gives a snapshot of the binding situation as it occurs in the incubation mixture and not in the final assay solution because of the slow extrusion of DNDGIC by 10 mM GSH (see "Results"). The inhibition of the low affinity binding site was followed by incubating variable amounts of DNDGIC (from 0.1 to 10 μM) with 40 nM of GSTs (20 nM for GSTM2-2) in 1 ml of 0.1 M potassium phosphate buffer, pH 7.4. After 5 min, the pH was adjusted to 6.5, and the concentration of GSH was brought to 10 mM, and 1 mM of CDNB was added rapidly. Residual activity was determined within 10 s from addition of substrates. GSTT2-2 (1.5 μM) was incubated at 37 °C with variable amounts of DNDGIC (from 0.75 to 15 μM) in 1 ml of 0.1 M potassium phosphate buffer, pH 7.4. After 10 min, 10 mM GSH and 0.25 mM menaphthyl sulfate (Msu) were added for activity measurements at 298 nm (38). GSTB1-1 (1 μM) was incubated at 25 °C with variable amounts of DNDGIC (from 0.75 to 15 μM) in 1 ml of 0.1 M potassium phosphate buffer, pH 7.4. After 10 min, the pH was adjusted to 6.5, and 10 mM GSH and 1 mM CDNB were rapidly added for activity measurements at 340 nm.

Inhibition experiments termed "under equilibrium conditions" were performed as described above with the exception that DNDGIC was incubated with each enzyme for 5 min (40 min for GSTT2-2) in the presence of a fixed GSH concentration (10 mM). After incubation with DNDGIC, aliquots were diluted in the assay mixture containing 10 mM GSH. After 5 min (40 min for GSTT2-2), 1 mM CDNB (1 mM menaphthyl sulfate for GSTT2-2) was added for activity determination. Data were fitted to a bi-exponential decay equation.

Fluorescence Experiments—Quenching of intrinsic fluorescence by DNDGIC was measured in a single photon counting spectrofluorometer (Fluoromax, S.A. Instruments, Paris, France) with a sample holder thermostatted at 25 °C (37 °C for GSTT2-2). Excitation was at 280 nm and emission at 340 nm. In a typical experiment GST (2 μM) was incubated with variable amounts of DNDGIC (from 0.2 to 20 μM) in 1 ml of 0.1 M potassium phosphate buffer, pH 7.4, containing 10 mM GSH and 1 mM GSNO. After 5 min (40 min for GSTT2-2), the fluorescence at 340 nm was measured and corrected for inner filter effect. Data were fitted to a bi-exponential decay equation.

Pre-steady State Kinetic Experiments—Rapid kinetic experiments were performed on a Applied Photophysics Kinetic spectrometer stopped-flow instrument equipped with a 1-cm light path observation chamber thermostatted at 25 °C (37 °C for GSTT2-2). In a typical experiment 4 μM GST in 0.1 M potassium phosphate buffer, pH 7.4, was rapidly mixed with an identical volume of the same buffer containing 5 μM DNDGIC, 20 mM GSH, and 2 mM GSNO. The reaction was followed by fluorescence changes at 320 nm (excitation at 280 nm; bandwidth 20 nm) and repeated at three different complex concentrations (5, 15, and 45 μM) and four different GSH (from 2 to 60 mM) and GSNO (from 0.2 to 6 mM) concentrations keeping the ratio GSH:GSNO constant at 10. Thousand data points were obtained on a logarithmic time scale. The experimental traces obtained at nine different DNDGIC and GSH (plus GSNO) concentrations were simultaneously fitted to Scheme 2 using the program Gepasi 3.21 (39–41). The program carries out the nonlinear minimization of the kinetic constants by means of numerical integration, at variable steps, of the ordinary differential equation according to Scheme 2,

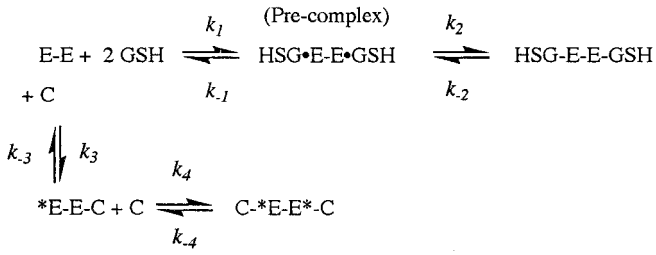

SCHEME 2

where *E* is each subunit with high affinity, *E** is the subunit with low affinity, *C* is DNDGIC, and *E*·GSH is the pre-complex found in the GSH binding mechanism to GSTA1-1, GSTP1-1, and GSTM2-2 (42). GSH binding to GSTT2-2 lacks the pre-complex intermediate (43).

EPR Experiments—Samples for EPR experiments were usually prepared in 0.1 M potassium phosphate buffer, pH 7.4, with DNDGIC added from a freshly made stock solution. EPR measurements were made at room temperature (22–25 °C) with a Bruker ESP300 X-band instrument (Bruker, Karlsruhe, Germany) equipped with a high sensitivity TM_{110}-mode cavity. To optimize instrument sensitivity, spectra were recorded using samples of 80 μl contained in flat glass capillaries (inner cross-section 5 × 0.3 mm) (44). For kinetics measurements standard round glass capillaries (1.10 mm inner diameter) with a working volume of 40 μl were applied, to allow rapid handling of samples. Unless otherwise stated spectra were measured over a 200 G range using 20 milliwatts power, 2.0 G modulation, and a scan time of 42 s; typically 4–40 single scans were accumulated to improve the signal to noise ratio. High resolution spectra were recorded with 0.1 G modulation and 2 milliwatts power. Simulation of anisotropic spectra was carried out using the SimFonia software provided by Bruker.

Radiometric Experiments—[^{3}H]GSH (glycine-2-^{3}H) (50 Ci/mmol) was purchased from PerkinElmer Life Sciences. [^{3}H]DNDGIC was prepared by reacting 20 mM [^{3}H]GSH (100 μCi/mmol) with 2 mM GSNO and 50 μM $FeSO_4$ in 1 ml (final volume) of 0.1 M potassium phosphate buffer, pH 7.4. After 30 min at 25 °C, [^{3}H]DNDGIC was quantitatively formed. GSTA1-1 (4 μM) was incubated with 2 μM [^{3}H]DNDGIC in the same buffer for 5 min. The amount of the complex bound to the high affinity

Downloaded from http://www.jbc.org/ by guest on July 18, 2018

site (more than 90%) was estimated on the basis of the observed inhibition. The solution was rapidly filtered on a Whitman 3MM filter paper. The filter was washed twice with 1 ml of cold buffer to remove excess of [^{3}H]GSH and of unbound [^{3}H]DNDGIC. The dried filter was dipped into 3 ml of Optifluor and, after 6 h, the radioactivity was determined by liquid scintillation spectrometry. Blank experiments, in the absence of $FeSO_4$ or GSTA1-1 were performed to evaluate the amount of spurious radioactivity retained by the filter or by the protein.

DNDGIC Exchange between GSTM2-2 and GSTA1-1—GSTM2-2 (2.5 μM) was reacted for 5 min with 1.25 μM DNDGIC in 0.1 M potassium phosphate buffer, pH 7.4. Residual activity determined with CDNB was 52% of the initial value. The enzyme was then added to an identical volume of the same buffer containing 2.5 μM GSTA1-1. By taking advantage of the different specific activities of GSTA1-1 and GSTM2-2 toward CDNB (80 and 200 units/mg, respectively) and NBD-Cl (40 and 3 units/mg, respectively), the concentration of the bound and free forms of each enzyme was calculated at fixed incubation times.

Molecular Modeling—Molecular modeling was performed by using the program Insight II (release 2000; MSI, San Diego). The models were based on the crystallographic coordinates of the different GSTs in complex with GSH, as obtained from the Brookhaven Protein Data Bank: A1-1, entry 1guh (2.6 Å resolution); M2-2, entry 1hna (1.85 Å resolution); P1-1, entry 6gss (1.9 Å resolution); and T2-2, entry 1ljr (3.2 Å resolution). The procedure followed was very similar to that already reported for GST P1-1 (18); the GSH-dinitrosyl-iron complex model was docked in the active site of the enzyme by assuming that the GSH molecule was in the same position and conformation as in the crystal structure of the enzyme-GSH complex. After adding the iron atom and the two NO molecules by assuming a tetrahedral geometry for the complex, it was immediately evident that the hydroxyl moiety of a Tyr or Ser residue (Tyr-9 in GST A1-1, Tyr6 in M2-2, Tyr-7 in P1-1, and Ser-11 in T2-2) was always at the appropriate distance and orientation to act as the fourth ligand of the iron atom, and therefore this coordination bond was added. Bond distances and angles were determined by the Builder module of the Insight II program. Finally the model was energy-minimized to convergence while keeping all the protein atoms fixed (except those of the Tyr or Ser residue), using the Discover module of Insight II and the CVFF force field (45). For comparison purposes, a similar minimization was performed also for the GSH molecule in the crystallographic enzyme-GSH complex. Graphic representation of the final model was produced by the program MOLMOL (46).

RESULTS

Inhibition Experiments—In a first experimental approach, the interaction of DNDGIC with representative members of the GST superfamily was studied on the basis of the competitive inhibition by DNDGIC. Under the experimental conditions used previously for GSTP1-1 (18), the inhibition of GSTM2-2 at variable DNDGIC concentrations shows a biphasic behavior close to that found for GSTP1-1, suggesting a similar cooperative mechanism that lowers the affinity of the vacant subunit for DNDGIC (Fig. 1). Binding to the high affinity G-site is so efficient that low amounts of DNDGIC inhibit stoichiometrically up to about 50% of the original activity. Because it is not possible to determine the trace amounts of free complex in solution in this first phase, only an apparent upper limit value of $K_{i1} \leq 10^{-11}$ M can be estimated for the high affinity binding site, whereas the affinity of the low affinity binding site can be calculated more accurately ($K_{i2} = 1.3 \times 10^{-8}$ M). The cooperative mechanism triggered by DNDGIC binding does not modify the affinity for GSH as suggested by an unchanged K_m value found in half-inactivated GSTM2-2 (data not shown). The Alpha class GSTA1-1 also shows strong affinity (apparent $K_{i1} \leq 10^{-11}$ M), but only 10% of the total activity remains when one active site of the dimeric protein binds one DNDGIC (Fig. 1). Because of the very low residual activity of the second subunit, only an approximate K_{i2} value of about 10^{-8} M can be evaluated for the low affinity binding site. The inhibition of the vacant active site is not caused by a change of affinity for GSH. In fact, the half-complexed enzyme with DNDGIC shows an unchanged K_m value for GSH (0.18 mM). A negative influence of DNDGIC bound to one subunit on the deprotonation of GSH (crucial in catalysis) in the adjacent subunit is also unlikely. In fact, the k_{cat} *versus* pH plot overlaps that found for the native enzyme, showing that the pK_a value of GSH is unchanged (experiments not shown). Thus, unproductive binding of GSH is possibly involved in the observed overinhibition. GSTT2-2 shows a different behavior. This enzyme, probably developed before Alpha, Pi, and Mu class GSTs in the evolutionary pathway (43, 47), shows a small and buried G-site, and a Ser residue (Ser-11) replaces the Tyr residue found in the more recently evolved GSTs which is essential for the activation of the bound GSH. GSTT2-2 displays a hundred times lower affinity for DNDGIC (apparent $K_{i1} \leq 4 \times 10^{-6}$ M, Fig. 1), whereas the biphasic inhibition pattern suggests a similar negative cooperativity. The high concentration of enzyme used in these kinetic experiments (due to the very low specific activity of GSTT2-2) and the low concentration of the DNDGIC stock solution do not allow measurement of reliable K_{i2} values for the low affinity binding site. Interestingly, the bacterial GSTB1-1, which binds GSH with low affinity and lacks a Tyr or Ser residue for GSH

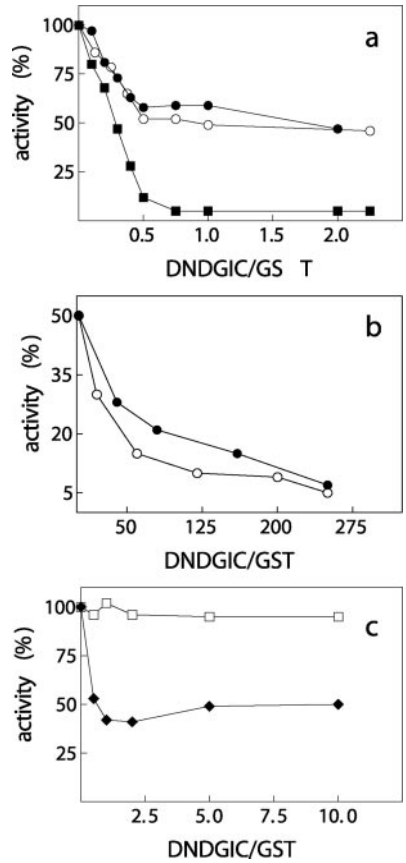

FIG. 1. **Inhibition of different GST isoforms by DNDGIC.** *a*, DNDGIC (from 0.4 to 9 μM) was incubated with 4 μM GSTP1-1 ○, GSTM2-2 ●, and GSTA1-1 ■ in 0.1 M potassium phosphate buffer, pH 7.4, at 25 °C. After 2 min of incubation, 4-μl aliquots (10 μl for GSTM2-2) were diluted in 1 ml of 0.1 M potassium phosphate buffer, pH 6.5, containing 10 mM GSH and 1 mM CDNB for activity measurements. *b*, GSTP1-1 (40 nM) ○ and GSTM2-2 (20 nM) ● were incubated in 1 ml of 0.1 M of potassium phosphate buffer, pH 7.4, with variable amounts of DNDGIC (from 0.1 to 10 μM). After 2 min, the pH was adjusted to pH 6.5; the GSH concentration was brought to a final concentration of 10 mM, and 1 mM CDNB was then added for activity measurement. *c*, GSTT2-2 ♦ (1.5 μM) and GSTB1-1 □ (1 μM) were incubated at pH 7.4 (25 °C for GSTB1-1 and 37 °C for GSTT2-2) with variable amounts of DNDGIC (from 0.75 μM to 15 μM). After 10 min the pH was adjusted to 6.5 for GSTB1-1, and activity measurements were done by adding 10 mM GSH and 1 mM CDNB (25 °C). Activity measurements for GSTT2-2 were performed at pH 7.4 (37 °C) after addition of 10 mM GSH and 0.25 mM Msu. Activity is expressed as percentage of the original value.

Downloaded from http://www.jbc.org/ by guest on July 18, 2018

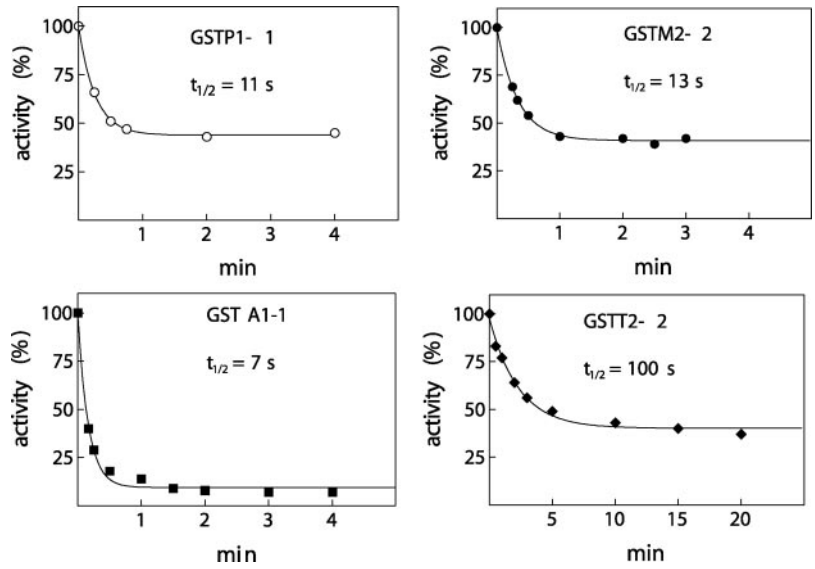

FIG. 2. **Kinetics of inhibition of GSTA1-1, GSTM2-2, GSTP1-1, and GSTT2-2.** 2 μM GSTP1-1 ○, GSTM2-2 ●, and GSTA1-1 ■ were incubated with 2 μM of DNDGIC and 1 mM GSH in 1 ml of 0.1 M potassium phosphate buffer, pH 7.4 (25 °C). At fixed times, 10-μl aliquots were assayed for activity at pH 6.5 in the presence of 10 mM GSH and 1 mM CDNB. GSTT2-2 ♦ (2 μM) was incubated at 37 °C with 2 μM DNDGIC and 1 mM GSH in 0.1 M potassium phosphate buffer, pH 7.4. At fixed times the GSH concentration was brought to 10 mM, and 0.25 mM Msu was added for activity assay. Activity is expressed as percentage of the initial value.

activation, shows an unchanged activity even in the presence of 10 moles excesses of DNDGIC (Fig. 1), indicating that this more primitive enzyme has scarce affinity for this complex.

Apparently all inhibition experiments reported above gave reliable data, but caution must be taken in kinetic studies involving tight binding inhibitors. It is not unusual that they need minutes and sometimes hours to reach steady state conditions. Thus, further analysis is required to check possible occurrence of slow reacting species in the DNDGIC-GST system.

DNDGIC Binding and Extrusion from the Active Site Are Slow Events—Binding of stoichiometric amounts of DNDGIC to the G-site of all representative GST members is a relatively slow event. As expected on the basis of a reciprocal competition of GSH and DNDGIC for the same G-site, the presence of increasing concentrations of GSH lowers the rate of the binding process and the extent of the final inhibition. By using 1 mM GSH, 2 μM enzyme, and 2 μM DNDGIC, kinetics of binding has $t_{1/2}$ values of 7, 13, and 11 s for GSTA1-1, GSTM2-2, and GSTP1-1, respectively (Fig. 2). GSTT2-2 exhibits the lowest rate of DNDGIC binding with a $t_{1/2}$ of 100 s (Fig. 2). In the presence of 10 mM GSH (the highest GSH concentration present in our kinetics experiments), a reasonable equilibrium (*i.e.* constant inhibition) is reached only after 5 min of incubation for Alpha, Pi, and Mu GSTs (25 °C), whereas 40 min are required for GSTT2-2 at 37 °C (data not shown). Displacement of DNDGIC by GSH is also a slow process. When the enzyme is first reacted with DNDGIC in 1 mM GSH and then incubated with 10 mM GSH, a time-dependent partial reactivation occurs, characterized by $t_{1/2}$ values of 40 s for GSTA1-1 and GSTP1-1, 80 s for GSTM2-2, and 1000 s for GSTT2-2 (data not shown). Kinetics of reactivation does not change by varying the final GSH concentration from 5 to 20 mM, and this means that GSH binding is rate-limited by the release of the complex from the G-site. In other words, apparent $k_{\text{reactivation}}$ values may be assumed to correspond to the apparent k_{off} values of the competitive inhibitor. These kinetic findings suggested conditions to be used for inhibition experiments under equilibrium conditions (see "Experimental Procedures"). Under these new assay conditions, negative cooperativity is still evident for GSTM2-2, GSTP1-1, and GSTT2-2, and more accurate K_i values can be calculated (Fig. 3 and Table I) in the presence of constant 10 mM GSH concentration. GSTA1-1 displays the highest affinity ($K_{i1} = 8.0 \times 10^{-11}$), and a similar K_{i1} value of about 1.0×10^{-9} M has been found for the high affinity binding site of Pi and Mu

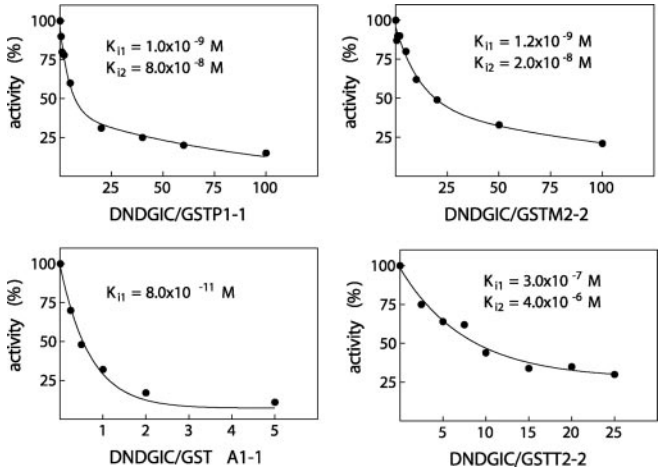

FIG. 3. **Inhibition of different GST isoforms by DNDGIC under equilibrium conditions.** GSTA1-1, GSTM2-2, and GSTP1-1 were incubated for 5 min with variable amounts of DNDGIC at pH 7.4 in the presence of 10 mM GSH as described under "Experimental Procedures." Aliquots were then diluted in the assay mixture containing 10 mM GSH. After 5 min of incubation, 1 mM CDNB was added for activity determination. The final enzyme concentration in the assay was 40 nM (20 nM for GSTM2-2). GSTT2-2 (1.5 μM) was incubated at pH 7.4 and 37 °C with variable amounts of DNDGIC (from 3.7 to 37 μM) and constant GSH (10 mM). After 40 min 0.25 mM Msu was added for activity assay. *Continuous lines* are the best fit of the experimental points obtained for GSTP1-1, GSTM2-2, and GSTT2-2 to a bi-exponential decay equation. The *continuous line* for GSTA1-1 is the best fit to a monoexponential decay equation. K_{i1} and K_{i2} represent the inhibition constants for the high and low affinity binding sites.

GSTs (8.0×10^{-8} and 2.0×10^{-8} M for their low affinity binding sites, respectively). The Theta GSTT2-2 shows the lowest affinity with $K_{i1} = 3.0 \times 10^{-7}$ M and $K_{i2} = 4.0 \times 10^{-6}$ M.

We must emphasize that the kinetic data obtained under "non-equilibrium" conditions, *i.e.* without a preincubation step of the inhibited enzyme with 10 mM GSH in the assay mixture, are of particular interest. Because of the slow reactivation kinetics by 10 mM GSH, they provide a snapshot of the DNDGIC-GST interaction as it occurs immediately after exposure to the complex and not in the final assay mixture. This allows us to evaluate the binding stoichiometry (see Fig. 1) involving the high affinity G-site and to check the interaction of DNDGIC with GSTs in heterogeneous biological systems as described in the accompanying paper (48).

Downloaded from http://www.jbc.org/ by guest on July 18, 2018

TABLE I

Kinetic and thermodynamic parameters for DNDGIC binding to GSTs

Details of inhibition, fluorescence, and stopped-flow experiments are given in the text.

	Inhibition data (M)	Fluorescence data (M)	Stopped flow data
GSTA1–1 (25 °C)	$K_{i1} = 8.0 \times 10^{-11}$	$K_{D1} \leq 5.0 \times 10^{-10}$	$k_{on} = 4.9 (\pm 0.5) \times 10^{7}$ M^{-1} s^{-1} $K_{D1} = 2.0 \times 10^{-10}$ M $k_{off} = 1.0 (\pm 0.1) \times 10^{-2}$ s^{-1}
		$K_{D2} = 3.4 \times 10^{-9}$	$k_{on} = 2.5 (\pm 0.3) \times 10^{5}$ M^{-1} s^{-1} $K_{D2} = 4.0 \times 10^{-8}$ M $k_{off} = 1.0 (\pm 0.1) \times 10^{-2}$ s^{-1}
GSTP1–1 (25°C)	$K_{i1} = 1.0 \times 10^{-9}$	$K_{D1} \leq 1.0 \times 10^{-9}$	$k_{on} = 1.0 (\pm 0.8) \times 10^{7}$ M^{-1} s^{-1} $K_{D1} = 2.0 \times 10^{-9}$ M $k_{off} = 2.0 (\pm 0.1) \times 10^{-2}$ s^{-1}
	$K_{i2} = 8.0 \times 10^{-8}$	$K_{D2} = 8.0 \times 10^{-8}$	$k_{on} = 3.2 (\pm 0.3) \times 10^{5}$ M^{-1} s^{-1} $K_{D2} = 6.2 \times 10^{-8}$ M $k_{off} = 2.0 (\pm 0.1) \times 10^{-2}$ s^{-1}
GSTM2–2 (25°C)	$K_{i1} = 1.2 \times 10^{-9}$	$K_{D1} \leq 5.0 \times 10^{-10}$	$k_{on} = 4.1 (\pm 0.3) \times 10^{6}$ M^{-1} s^{-1} $K_{D1} = 1.4 \times 10^{-9}$ M $k_{off} = 5.6 (\pm 0.1) \times 10^{-3}$ s^{-1}
	$K_{i2} = 2.0 \times 10^{-8}$	$K_{D2} = 8.0 \times 10^{-8}$	$k_{on} = 3.0 (\pm 0.3) \times 10^{5}$ M^{-1} s^{-1} $K_{D2} = 1.9 \times 10^{-8}$ M $k_{off} = 5.6 (\pm 0.1) \times 10^{-3}$ s^{-1}
GSTT2–2 (37°C)	$K_{i1} = 3.0 \times 10^{-7}$	$K_{D1} \leq 3.0 \times 10^{-7}$	$k_{on} = 3.0 (\pm 0.1) \times 10^{3}$ M^{-1} s^{-1} $K_{D1} = 2.0 \times 10^{-7}$ M $k_{off} = 6.0 (\pm 0.1) \times 10^{-4}$ s^{-1}
	$K_{i2} \cong 4.0 \times 10^{-6}$	$K_{D2} \cong 5.0 \times 10^{-6}$	$k_{on} = 4.0 (\pm 0.3) \times 10^{2}$ M^{-1} s^{-1} $K_{D2} \cong 1.5 \times 10^{-6}$ M $k_{off} = 6.0 (\pm 0.1) \times 10^{-4}$ s^{-1}

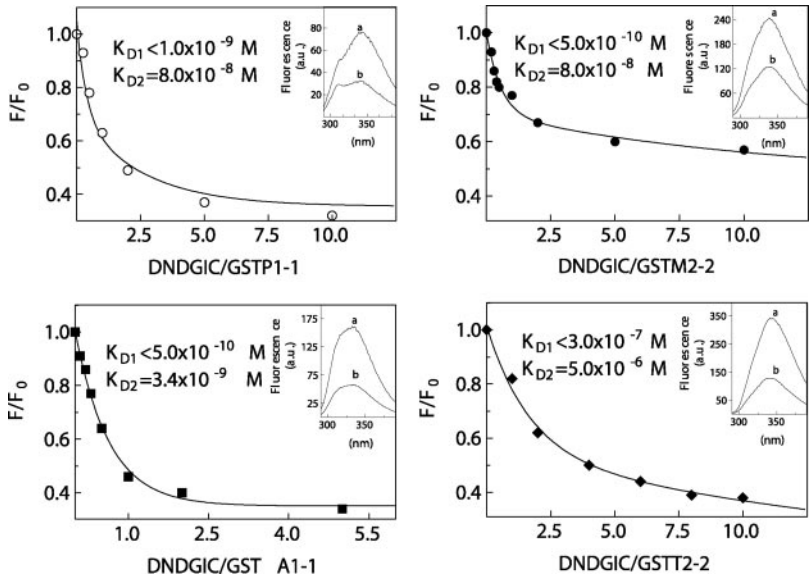

FIG. 4. **Isothermic binding of DNDGIC to different GST isoforms.** Isothermic binding of DNDGIC to GSTs (2 μM) has been studied at 25 °C (37 °C for GSTT2-2) using the perturbation of the intrinsic fluorescence of the proteins (340 nm) at variable concentrations of DNDGIC (from 0.2 to 20 μM), 10 mM GSH, and 1 mM of GSNO, pH 7.4. Fluorescence measurements were done after 5 min of incubation (40 min for GSTT2-2). F is the intrinsic fluorescence at 340 nm after addition of DNDGIC plus GSH and GSNO; F_0 is the intrinsic fluorescence in the presence of GSH and GSNO. *Continuous lines* are the best fit of the experimental points to a bi-exponential decay equation. *Insets* show the fluorescence spectra of the enzymes (2 μM) in the 10 mM GSH and 1 mM GSNO (*curve a*) and in the presence of 20 μM of DNDGIC, 10 mM GSH and 1 mM GSNO (*curve b*).

Fluorescence Experiments—Binding of DNDGIC to GSTs causes a significant perturbation of the intrinsic fluorescence at 340 nm (Fig. 4), useful to estimate directly the thermodynamic dissociation constant of the DNDGIC-enzyme complex in the absence of CDNB as co-substrate. Fluorescence experiments have been carried out at fixed GSH and GSNO concentrations (10 and 1 mM, respectively), and the fluorescence quenching by DNDGIC was corrected for the fluorescence perturbation due to GSH and GSNO. Data reported in Fig. 4 fit well to a binding equation that includes one high affinity and one low affinity binding site (see Table I). Because of the relatively high concentrations of enzyme and complex used in these experiments, an almost stoichiometric binding of the inhibitor to the high affinity G-site has been found, so only an upper limit of the K_D value can be estimated. Interestingly, the fluorescence approach allowed us to visualize well the binding of DNDGIC to the low affinity G-site of GSTA1-1. This event could not be characterized accurately by inhibition experiments as the hemisaturated enzyme is almost inactive (see Fig. 1).

Stopped-flow Experiments—A more detailed and conclusive kinetic investigation on the binding of DNDGIC to the representative members of the GST superfamily has been done by stopped-flow experiments, by following the quenching of intrinsic fluorescence at 340 nm after rapid addition of DNDGIC to each enzyme (Fig. 5). The experimental traces obtained with a set of experiments, performed by rapid mixing of GSTA1-1, GSTM2-2, and GSTP1-1 with variable amounts of DNDGIC at constant GSH and GSNO concentrations, show two distinct phases. A first very fast fluorescence quenching due to the binding of GSH (or GSNO) to the G-site is followed by a slower fluorescence quenching attributed to the binding of the complex. Most of the first fast interaction of the enzyme with GSH is lost in the instrumental dead time and can be followed adequately only at 5 °C, thus being characterized by the same microscopic rate constants reported previously for the GSH binding (42, 43). Thus, the presence of DNDGIC (several orders of magnitude less concentrated than GSH) and GSNO (10 times less concentrated than GSH) seems to have no relevant effect on this first event, *i.e.* GSH binding. The second slower phase, *i.e.* DNDGIC displacing GSH, occurs on a very different time scale (Fig. 5). All experimental traces for GSTA1-1 and GSTP1-1 have been fitted well to a minimal binding mechanism (see Scheme 2) that includes a first interaction of GSH and GSNO to the G-site followed by a slower but thermodynamically favored bimolecular interaction of the free enzyme with DNDGIC. GSTM2-2 shows a small additional fluorescence

Downloaded from http://www.jbc.org/ by guest on July 18, 2018

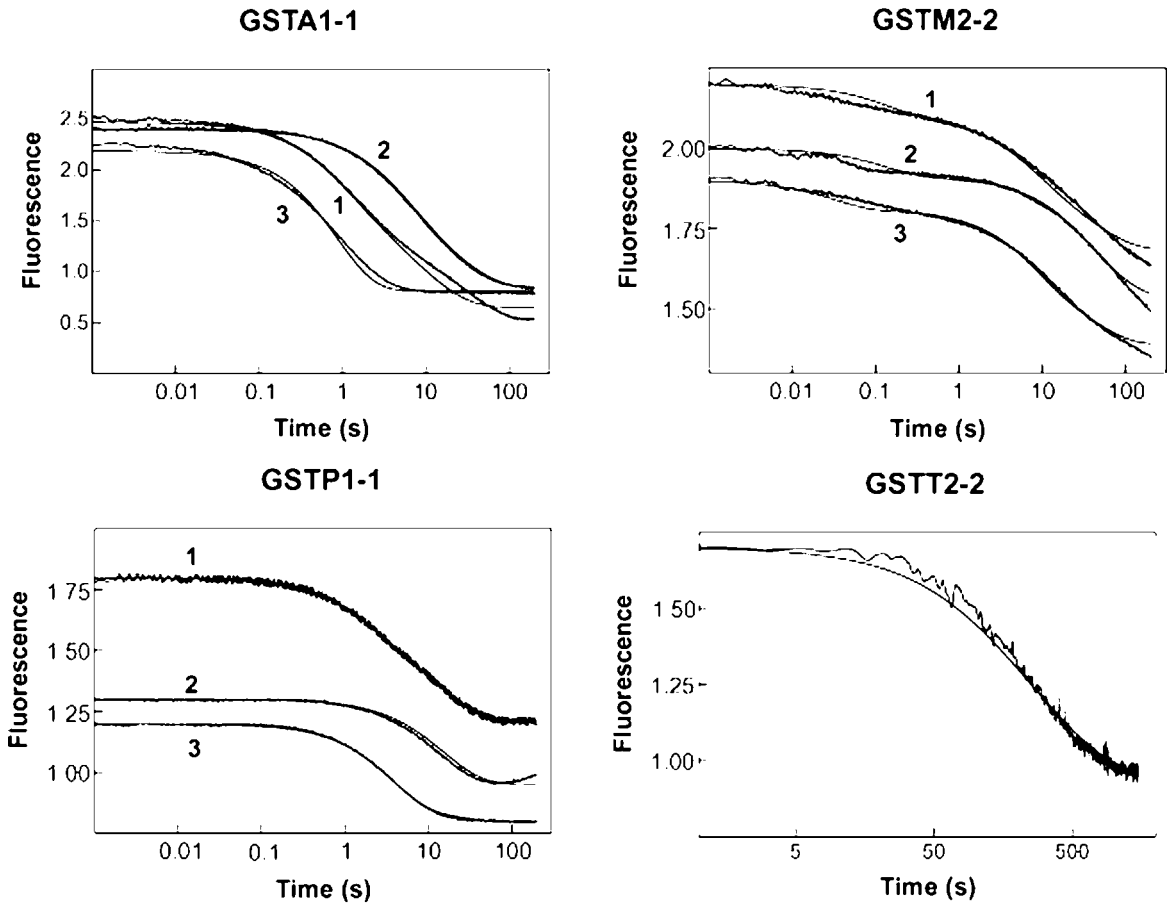

FIG. 5. **Stopped-flow kinetics of DNDGIC binding.** Stopped-flow experiments have been performed as described under "Experimental Procedures." A few representative traces are shown in each panel showing kinetics of quenching of intrinsic fluorescence at 25 °C (λ_{ex} = 280 nm, λ_{em} = 320 nm) due to DNDGIC binding to each enzyme and at variable GSH and GSNO concentrations. GSTA1-1, GSTM2-2, and GSTP1-1 (4 μM) (0.1 M potassium phosphate buffer, pH 7.4) were mixed with an identical volume of the same buffer containing the following: *trace 1,* DNDGIC (5 μM), GSH (2 mM), and GSNO (0.2 mM); *trace 2*, DNDGIC (5 μM), GSH (20 mM), and GSNO (2 mM); *trace 3,* DNDGIC (45 μM), GSH (20 mM), and GSNO (2 mM). GSTT2-2 (4 μM) was mixed with an identical volume of the same buffer containing DNDGIC (8 μM), GSH (6 mM), and GSNO (0.6 mM). Binding was followed at 37 °C by a traditional spectrofluorometer.

perturbation that occurs after GSH binding and before DNDGIC binding. This unknown event, which probably reflects a pre-complex formation, has not been detailed because the exclusion of this additional event in the minimal reaction Scheme 2 gives a satisfactory fit to all the experimental traces.

Because of its very slow rate, the interaction of GSTT2-2 with DNDGIC can be followed by a traditional spectrofluorometer (Fig. 5). Even in that case, the experimental traces fit well to Scheme 2, and this analysis confirms relatively low k_{on} values for both the high and low affinity G-sites (3.0×10^3 and 4.0×10^2 M^{-1} s^{-1}, respectively). The calculated microscopic kinetic constants and the overall equilibrium constants for all representative GST members shown in Table I are in good agreement with those obtained from inhibition data at equilibrium and from static fluorescence experiments.

EPR Data—The low resolution spectrum of free DNDGIC at room temperature shows a single symmetrical line at $g = 2.03$, typical of the rapid isotropic motion of a small molecule tumbling freely in aqueous solution (Fig. 6). Under high resolution conditions the single line can be seen to be a multiline signal; the spectrum is composed of 25 lines due to the hyperfine coupling of a single unpaired electron to 2 eq nitrosyl nitrogens and 4 eq methylene protons from the cysteines of the two bound glutathiones (Fig. 6, *inset*), in analogy to the similar dinitrosyl-dicysteinyl-iron complex (49). The EPR spectra of dinitrosyl-iron complexes in biological systems reported in the literature have almost always been obtained using frozen samples, typically measured at 77–100 K in order to take advantage of the enhanced instrument sensitivity at low temperatures. However, under these conditions both protein-bound and free dinitrosyl complexes are immobilized and give broad anisotropic signals covering approximately the same spectral range, making it difficult to single out the individual components of a sample containing different DNIC species. We have therefore carried out experiments at room temperature where the spectra of free and bound complexes can easily be distinguished.

When substoichiometric amounts of DNDGIC are added to GSTA1-1, only the spectrum of an enzyme-bound complex is observed (Fig. 6). Binding of the complex is too fast to be measured and is completed within the experimental dead time of less than 30 s. No free complex can be detected until more than 0.5 eq of DNDGIC per subunit is added. At higher stoichiometries only part of the complex binds to the second active site, and the signal of the free complex appears in the spectrum (Fig. 6). This result confirms that binding of the complex to one active site with high affinity drastically lowers the affinity for binding at the second active site. The spectrum of DNDGIC bound to the low affinity G-site appears to be identical to that of the high affinity active site (Fig. 6, *curve 4*). GSTP1-1 and GSTM2-2 give very similar results, demonstrating that the presence of a high affinity binding site for a dinitrosyl-iron complex is maintained in these three classes of GST, despite differences in their substrate specificity and active site geometry. Also the GSTT2-2 isoform is able to bind the dinitrosyl-

Downloaded from http://www.jbc.org/ by guest on July 18, 2018

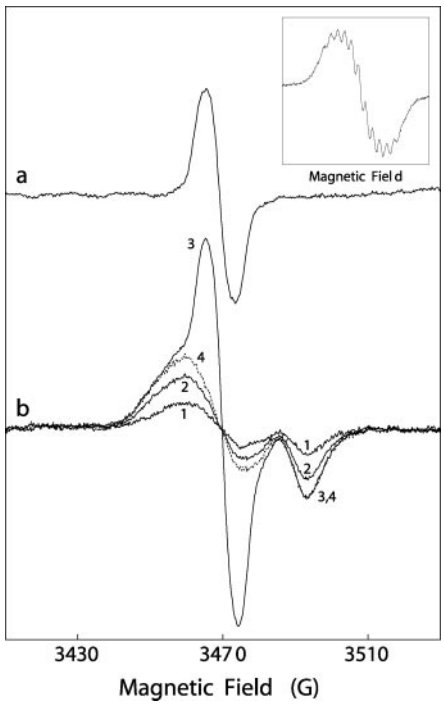

FIG. 6. **EPR spectra of free and bound dinitrosyl-iron complexes.** Spectrum *a*, 10 μM free DNDGIC in 0.1 M potassium phosphate buffer, pH 7.4, measured at room temperature (22–25 °C) under low resolution conditions with 8 scans accumulated. *Inset*, in the high resolution spectrum of the same sample, 40 scans were accumulated to achieve an acceptable signal to noise ratio. The spectra in *b* represent EPR titration of DNDGIC binding to GSTA1-1. GSTA1-1 (30 μM) in 0.1 M potassium phosphate buffer, pH 7.4, was reacted with 7.5 μM (*spectrum 1*), 15 μM (*spectrum 2*), or 30 μM (*spectrum 3*) of DNDGIC. The concentration of bound complex in spectra 1–3 was 7.5, 15, and 23 μM, respectively, as determined directly from height of the high field transition, whereas the free complex is only observed in spectrum 3 (7 μM). At high resolution the hyperfine splitting pattern of free DNDGIC could be observed in the central peak of spectrum 3 (not shown). The spectrum 3, subtracted from the spectral component of the free complex, reflects a 100% occupancy of DNDGIC to the high affinity G-site and 50% to the low affinity G-site (*spectrum 4*). The spectrum 4 shows a similar shape and maximum as in spectra 1 and 2 (50 and 100% occupancy of DNDGIC to the high affinity G-site) suggesting a structural equivalence of the two G-sites after binding of the complex.

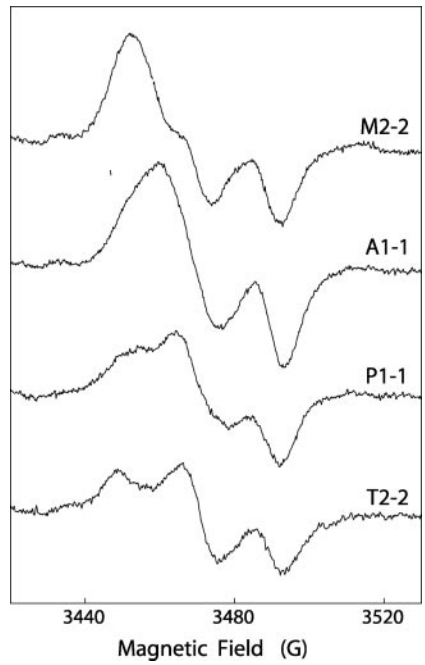

FIG. 7. **EPR spectra of DNDGIC bound to different GST isoforms.** The samples contained 30 μM of each enzyme and 15 μM DNDGIC in 0.1 M potassium phosphate buffer. With GSTT2-2, 15 μM enzyme and 7.5 μM DNDGIC were used; this sample was incubated for 1 h before EPR measurement.

TABLE II
Magnetic parameters (g-tensor) for DNDGIC bound to different GST isoenzymes

The values were determined through anisotropic simulation of EPR spectra measured at room temperature (22–25 °C); samples were prepared as in Fig. 7. Spectra were simulated using the same set of linewidth parameters: $Lw_x = Lw_y = 8$ G, $Lw_z = 12$ G.

GST isoform	g_x	g_y	g_z
A1-1	2.014	2.032	2.035
M2-2	2.015	2.036	2.037
P1-1	2.015	2.028	2.038
T2-2	2.014	2.027	2.041

iron complex with high affinity, but in this case the rate of binding is extremely slow. Interestingly, the spectrum of the GST-bound dinitrosyl-iron complexes changes appreciably according to the GST isoform used (Fig. 7). The A1-1 and M2-2 GSTs give essentially axial spectra, whereas P1-1 and T2-2 give strongly rhombic spectra, but there are minor differences in the spectra that in practice make it possible to identify the type of GST involved directly from the EPR spectrum. The *g* values were determined through an anisotropic simulation of the spectra (Table II); all four complexes show almost identical g_x values, whereas g_y and g_z values vary. The g_x transitions are well separated from the others, and computer analysis reveals they all have identical line widths and line shapes; this suggests that the differences observed in the spectra are caused by geometry changes and not by ligand substitution.

Radiometric Experiments—Previous findings (18) indicated that in the active site of GSTP1-1, after binding of DNDGIC and removal of the excess of GSH by passage through a G-25 Sephadex column, the iron ion is coordinated by one GSH, two NO, and the hydroxyl group of Tyr-7. It was unclear whether a second GSH molecule could act as a fifth ligand in the presence of an excess of GSH. In fact, subtle UV-visible and EPR spectral changes have been observed previously for the bound DNDGIC when the excess of GSH is removed by gel filtration (18). In an attempt to quantify the GSH molecules present in the GST-bound complex, we adopted a well known radiometric approach used to characterize the classical ligand-receptor interaction and based on rapid filtration of a radioactively labeled ligand-receptor mixture. The excess of labeled reagent is removed by filtration, whereas the ligand-protein complex is retained by the filter. This procedure has been used for GSTA1-1 (4 μM) after incubation with [^{3}H]DNDGIC (2 μM) in the presence of 0.8 mM [^{3}H]GSH. The amount of the bound DNDGIC (more than 90%) has been evaluated from the extent of the final inhibition. After rapid filtration, the recovered radioactivity bound to the enzyme indicates a strict one to one stoichiometry between GSH and the bound complex. Thus, the second GSH molecule of DNDGIC is no longer present in the bound complex (at 10 mM GSH) or is characterized by a very labile interaction with the iron atom. A possible explanation of the observed EPR spectral modification observed upon removal of the excess of GSH (18) could be found in a structural modification of the DNDGIC-bound subunit caused by the loss of GSH bound to the uninhibited active site of the adjacent subunit.

DNDGIC May Shift from GSTM2-2 to GSTA1-1—GSTM2-2 shows a specific activity about two times higher than GSTA1-1 when CDNB is used as co-substrate (200 and 80 units/mg, respectively). Conversely, GSTA1-1 can utilize efficiently NBD-Cl as second substrate (40 units/mg), whereas this com-

Downloaded from http://www.jbc.org/ by guest on July 18, 2018

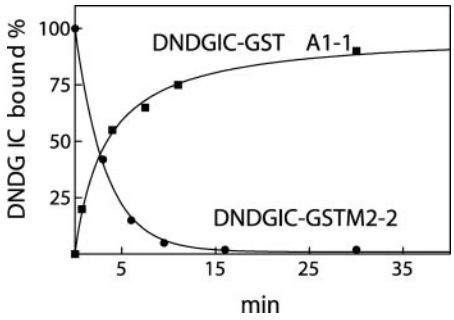

FIG. 8. **Shift of DNDGIC from GSTM2-2 to GSTA1-1.** GSTM2-2 (2.5 μM) was reacted for 5 min with 1.25 μM DNDGIC in 0.1 M potassium phosphate buffer, pH 7.4. Residual activity with CDNB was 51% of the initial value. The enzyme was then added to an identical volume of the same buffer containing 2.5 μM GSTA1-1. The amount of DNIC bound to each enzyme has been calculated at fixed times as described under "Experimental Procedures" and reported on the *ordinate*. ■, DNDGIC bound to GSTA1-1; ●, DNDGIC bound to GSTM2-2. The $t_{1/2}$ for displacement of DNDGIC from GSTM2-2 is very similar to that of DNDGIC binding to GSTA1-1 (2.8 and 3.2 min, respectively).

pound is a poor substrate for GSTM2-2 (3 units/mg). Based on the very different specific activities toward these substrates, it was possible to verify if DNDGIC, initially bound to GSTM2-2, can be transferred to the higher affinity GSTA1-1. The experiment reported in Fig. 8 clearly demonstrates that this really occurs. When GSTA1-1 is incubated in the presence of a hemicomplexed GSTM2-2 with DNDGIC, a time-dependent decrease of activity with NBD-Cl is observed, with a concomitant increase of activity with CDNB. This is direct evidence that DNDGIC is really transferred from the low affinity GSTM2-2 to the more strongly binding Alpha class GSTA1-1. The process shows a $t_{1/2}$ of about 3 min, compatible with the k_{off} of DNDGIC from GSTM2-2 (1–2 min).

Molecular Modeling—Fig. 9 shows molecular models of the GSH-dinitrosyl-iron complex in the active sites of the four different isoenzymes. As already shown for GST P1-1 (18), the Tyr residue conserved in the A1-1, M2-2, and P1-1 isoforms (1) is in the appropriate position to act as the fourth ligand of the iron atom (together with the GSH sulfur atom and the two NO molecules), probably displacing the second GSH.

In this geometry, the complex is partially exposed to the solvent and fits perfectly to the active site, because no van der Waals violations are observed and the total interaction energy is very favorable. In particular, −200, −240, −120, and −300 kcal/mol have been calculated for GSTA1-1, GSTM2-2, GSTP1-1, and GSTT2-2, respectively. These values represent the sum of Coulomb and van der Waals interaction terms between ligand and protein in the binary complex, and they do not take into account the interactions of these molecules with water (neither in the bound nor in the free state). The corresponding energies for GSH binding are similar, suggesting that the large difference in binding constants observed for the two ligands (GSH and DNDGIC) is ascribable mainly to the formation of the bond between the hydroxyl moiety of the Tyr or Ser side chain and the iron atom of the complex. This would explain the lack of affinity observed for the bacterial GST which has no Ser or Tyr residues at hydrogen bonding distance of the sulfur atom of GSH. The GSH structure is very similar in the models of the complex in the active sites of GST A1-1, M2-2, and P1-1 and does not differ appreciably from the conformation observed in the crystallographic enzyme-GSH structures. On the other hand, the GSH molecule adopts a significantly different conformation in the T2-2 isoenzyme, and the complex is mostly obscured by the extra C-terminal extension of about 40 residues which is a peculiar structural feature of this enzyme (16). However, both GSH and DNIC appear greatly stabilized in the G-site of GSTT2-2 giving even lower energy than that found in the more recently evolved GSTs. The partial exposition of the iron atom in the Alpha, Pi, and Mu class GSTs allows the presence of a second GSH molecule as a fifth iron ligand without relevant van der Waals violations (not shown), but this additional ligand cannot be located in the G-site of GSTT2-2 due to steric hindrance.

DISCUSSION

DNDGIC behaves like a tight binding inhibitor for all members of the human GST superfamily tested, *i.e.* GSTA1-1, GSTM2-2, GSTP1-1, and GSTT2-2. A first kinetics approach, which did not take into account the existence of slow-reacting species, gave an overestimation of the affinity of these enzymes for DNDGIC with apparent K_i values in the range of 10^{-10}–10^{-12} M. An overestimated $K_i \leq 10^{-11}$ M has been also reported previously for GSTP1-1 (18). More appropriate inhibition experiments under equilibrium conditions give reliable K_i values that range from 10^{-10} M for GSTA1-1, 10^{-9} M for GSTM2-2, and GSTP1-1 to 10^{-7} M for GSTT2-2 (Table I). Close to these values are the thermodynamic dissociation constants calculated from static fluorescence experiments (Table I) which also indicate that the binding of the co-substrate CDNB does not affect this process. These K_i values are far from those reported for other GST inhibitors; a lot of GSH derivatives act as competitive inhibitors for GSTs, but their dissociation constants for the G-site are only in the range of 10^{-4} to 10^{-5} M (50). Thus, to our knowledge, DNDGIC represents the most potent competitive inhibitor of GSTs acting on the strictly conserved G-site.

All inhibition and fluorescence data at equilibrium indicate also the presence of a high and a low affinity binding site in these GSTs. Because of the homodimeric structure of all these enzymes, negative cooperativity triggered by DNDGIC binding is likely involved. This is the first evidence of a common intersubunit communication operating in the GST superfamily which, in this case, lowers 10–100 times the affinity for the complex in the vacant subunit. Interestingly, in half-site complexed GSTs both the affinity of the adjacent G-site for GSH and its catalytic competence are unchanged, except for GSTA1-1 which lowers its catalytic activity of the second subunit to about 10%. Possibly unproductive binding of GSH causes such overinhibition.

Stopped-flow data fit well to a minimal binding mechanism common to all these GSTs (see Scheme 2), which includes a first interaction with GSH, according to the binding mechanisms described previously (42, 43), and a slower bimolecular interaction of DNDGIC with the high and low affinity G-sites (Table I). The overall K_D values calculated from the kinetic experiments are close to those given by equilibrium experiments (Table I). A careful examination of the microscopic rate constants gives additional information. It appears that DNDGIC binds to GSTA1-1, GSTM2-2, and GSTP1-1 with k_{on} values similar to those found for GSH (10^6–10^7 M^{-1} s^{-1}) (42), suggesting that the G-site is open enough to accommodate DNDGIC without gross structural changes. This agrees completely with molecular modeling data that show DNDGIC partially exposed to the solvent and well stabilized in the G-sites of these GSTs. The observed strong affinity is likely due to the coordination of the iron atom to the phenolate group of the conserved Tyr residue of the active site (Tyr-7 in GSTP1-1, Tyr-6 in GSTM2-2, and Tyr-9 in GSTA1-1) which also causes a very slow extrusion of the complex from the G-site (low k_{off} value). A lower k_{on} value for DNDGIC binding appears to be the kinetic determinant of the decreased affinity of the second G-site in the half-saturated GSTs. Thus, negative cooperativity is not caused by a non-optimized geometry of iron ligands in the second G-site (which would cause an increased k_{off} value) but

Downloaded from http://www.jbc.org/ by guest on July 18, 2018

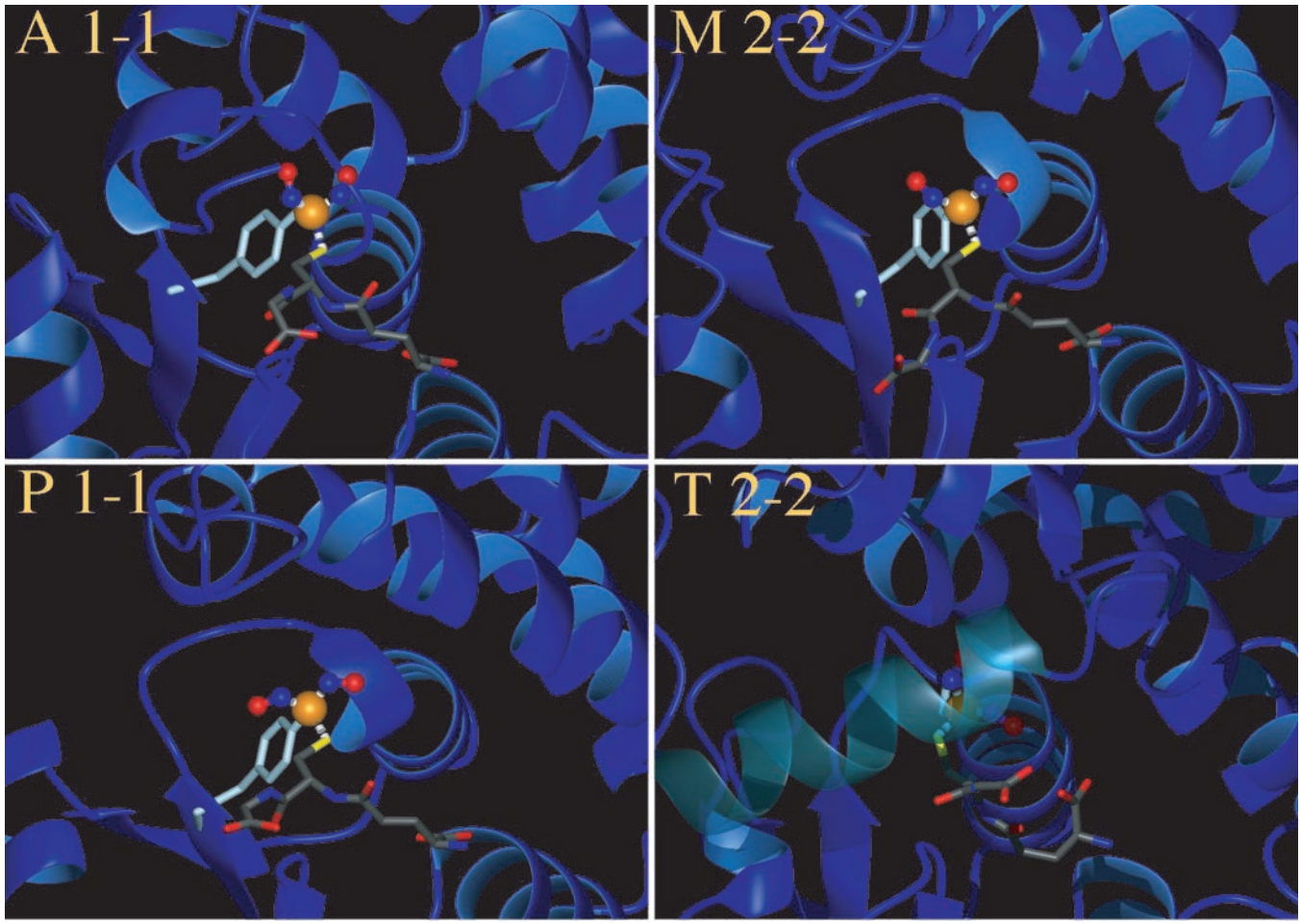

FIG. 9. **Molecular modeling.** Molecular modeling of DNDGIC in the active site of GSTA1-1, GSTM2-2, GSTP1-1, and GSTT2-2 was performed as described under "Experimental Procedures." The G-site is shown as a ribbon model, whereas crucial residues involved in the iron coordination (Tyr-9 in A1-1, Tyr-6 in M2-2, Tyr-7 in P1-1, and Ser-11 in T2-2) are shown as *sticks,* and the complex is reported as a "*ball* and *stick*" representation. The extra C-terminal segment which almost obscures the complex in GSTT2-2 is shown as a transparent helix. The iron atom is depicted as an *orange sphere*; the sulfur atom is colored *yellow*; and the oxygen is *red*. The figure was drawn using MolMol (46).

probably by an increased rigidity or shielding of the second G-site triggered by DNDGIC binding to the first subunit.

Kinetics data also indicate that once the G-site has bound DNDGIC, GSH can bind only when DNDGIC leaves the G-site (k_{on} for GSH binding = k_{off} for DNDGIC). This ruled out the possibility that the partial displacement of DNDGIC by an excess of GSH may occur through a transfer of the dinitrosyl-iron moiety from the bound DNDGIC to the free GSH. On the other hand, the mutual competition between GSH and DNDGIC for the G-site makes unlikely the possibility that the complex may be assembled in the active site by transfer of the dinitrosyl-iron moiety from the free DNDGIC to the bound GSH. However, an interesting observation is that DNDGIC may be easily translated from a low affinity GST enzyme (GSTM2-2) to a high affinity isoenzyme (GSTA1-1) (see Fig. 8). The kinetics of this event corresponds to the kinetics of DNDGIC release from the active site, so the exchange probably occurs by a simple binding of the released complex by the higher affinity enzyme. Finally, stopped-flow data give a rationale for the relatively scarce affinity of the Theta class GSTT2-2 for DNDGIC ($K_D = 10^{-7}$ M). In this enzyme, both k_{on} and k_{off} values of DNDGIC are small when compared with those of other GSTs, but k_{on} is 3–4 orders of magnitude lower, whereas k_{off} is only 10–100 times lower. Thus, a low k_{on} value appears to be the main determinant for the decreased affinity of GSTT2-2 for DNDGIC. This slow binding event could be due either to a shielded active site or to the necessity of a small structural change in order to allow the coordination of the iron atom by the hydroxyl group of Ser-11. Molecular modeling shows DNDGIC almost completely covered by the C-terminal extension which mostly obscures the G-site (see Fig. 9), whereas Ser-11 is in a proper position for iron coordination. The high negative value of energy for the complex in the G-site of GSTT2-2 and a low k_{off} value (even lower than those found for the other GSTs) are convincing indications that the coordination in the G-site is still efficient. How is it possible to explain the coexistence of a relatively scarce affinity of GSTT2-2 for the complex with a good stabilization of DNDGIC in the G-site? The molecular modeling results show that the restricted dimensions of the GSTT2-2 G-site makes it difficult for DNDGIC to enter. In addition, it has been shown that in GSTT2-2 a rapid equilibrium exists between at least two G-site conformations, E_1 and E_2 (43). Only the less populated conformation (E_2) is efficient in GSH binding, and this situation possibly occurs also for DNDGIC binding. Thus, DNDGIC binding to GSTT2-2 may be summarized as shown in Scheme 3,

$$E_1 \rightleftarrows E_2$$
$$E_2 + \mathrm{C} \underset{k_{off}}{\overset{k_{on}}{\rightleftharpoons}} E_2 - \mathrm{C}$$

SCHEME 3

Downloaded from http://www.jbc.org/ by guest on July 18, 2018

It is evident that, in case of a fast but unfavorable equilibrium toward E_2, the apparent k_{on} value is low and the overall thermodynamic dissociation constant would be relatively high, just as we found experimentally.

The total absence of any interaction of the bacterial GSTB1-1 with DNDGIC can be easily explained. This enzyme shows a Cys residue (Cys-10) instead of Tyr or Ser residues in a proper distance from the sulfur atom of GSH (16, 51). In addition, the native enzyme displays an unusual mixed disulfide involving Cys-10 and the bound GSH which rapidly exchange with a second GSH molecule transiently present in the G-site (52, 53). Thus no thiolate groups can act as ligands for the iron atom of DNDGIC.

Radiometric and EPR data provide more information about the way DNDGIC is bound to GSTs. In fact, experiments of rapid filtration after [^{3}H]DNDGIC incubation show that a second GSH molecule is not present as the fifth ligand of the iron in the G-site. So far no crystal structures of paramagnetic DNICs have been reported, but the free complex with two NO and two GSH ligands is believed to be pseudo-tetrahedral and gives a highly axial EPR spectrum in solution when immobilized at low temperatures (18). Surprisingly, the EPR spectra of the GST-bound dinitrosyl-iron complexes are different for all the GST isoforms studied. These differences indicate changes in the geometry of the ligand arrangement around the iron or in the nature of the ligands themselves but not in the number of ligands (four). Thus, assuming a four-coordinated iron with the ligand set [N, N, S^-, O^-] in the bound complex (as also suggested by the radiometric experiments reported in this paper), the axial spectra are consistent with a flattened, relatively symmetrical tetrahedral geometry for GSTM2-2 ($g_y = g_z$) and a more asymmetrical tetrahedral geometry for GSTA1-1 ($g_y = g_z$). In contrast, the rhombic spectra of P1-1 and T2-2 ($g_x \neq g_y \neq g_z$) indicates a very distorted structure of the bound complex in these GST isoforms. Because the A1-1, M2-2, and P1-1 show similar K_D values for DNDGIC, the actual conformation of the bound complex is therefore not important for the stability, as long as the iron is coordinated efficiently to both the glutathione and a tyrosine residue. Studies on dinitrosyl-iron complexes containing different ligands have shown that this type of complexes can adapt a wide range of structures, depending on the constraint induced by the two other ligands attached (54). We conclude that dinitrosyl-iron complexes are firmly bound to these GST isoforms through the glutathione thiolate-iron-tyrosinate ligand arrangement; constant S—Fe–O bond angles and bond lengths are essential for the high affinity, whereas the positions of the NO groups, which do not seem to contribute much to binding, will be determined by the space available in the active site of the enzyme. This is in agreement with the molecular modeling results as can be seen from Fig. 9.

The GSTT2-2 could be a case apart as a serine residue replaces the tyrosine residue in the iron coordination. However, EPR spectra show a geometry of the bound complex very similar to that found in GSTP1-1. Thus, the reason for the slow binding of DNDGIC must be found in the difficult access to the G-site and not in a scarce stabilization in the active site, as suggested above on the basis of kinetic and molecular modeling data.

Finally, EPR data add further details concerning the cooperative mechanism. In fact, the ligand configurations of DNDGIC are identical in the hemi-saturated and in the fully saturated enzyme, because occupation of the second site does not give rise to the appearance of a second species in the EPR spectrum (see Fig. 6). The sequential mechanism (KNF) is the sole model that accounts for negative cooperativity. This model assumes a symmetric structure in the fully complexed enzyme but an asymmetric state (T-R) in the hemi-complexed enzyme. However, this situation is not confirmed by our EPR data. Alternatively, negative cooperativity may be explained on the basis of a change of flexibility or accessibility of the G-site. In that case, binding of the ligand to the first subunit would lower the accessibility to the free adjacent subunit with consequent lowering of affinity but without changing the topography of the active site. This possibility agrees well with our kinetics and EPR results.

The data reported in this paper allow interesting conclusions from an evolutionary point of view. It is accepted that the Theta class GSTT2-2 is close to the ancestral precursor of all GSTs (43), whereas GSTA1-1, GSTM2-2, and GSTP1-1 are believed to be more recently evolved enzymes. It appears that the GST superfamily is under evolutionary pressure in the direction of the optimization of the binding process of DNDGIC, and this may be related to the increasing physiological relevance of nitric oxide during evolution. In fact, only eukaryote organisms are able to use NO efficiently as chemical messenger, although the role of NO in prokaryotes remains to be solved.

REFERENCES

1. Armstrong, R. N. (1997) *Chem. Res. Toxicol.* **10,** 2–18
2. Mannervik, B., Ålin, P., Guthenberg, C., Jensson, H., Tahir, M. K., Warholm, M., and Jornvall, H. (1985) *Proc. Natl. Acad. Sci. U. S. A.* **82,** 7202–7206
3. Meyer, D. J., Coles, B., Pemble, S. E., Gilmore, K. S., Fraser, G. M., and Ketterer, B. (1991) *Biochem. J.* **274,** 409–414
4. Buetler, T. M., and Eaton, D. L. (1992) *Environ. Carcinog. Ecotoxicol. Rev.* **10,** 181–200
5. Meyer, D. J., and Thomas, M. R. (1995) *Biochem. J.* **311,** 739–742
6. Pemble, S. E., Wardle, A. F., and Taylor, J. B. (1996) *Biochem. J.* **319,** 749–754
7. Board, P. G., Baker, R. T., Chelvanayagam, G., and Jermiin, L. S. (1997) *Biochem. J.* **328,** 929–935
8. Board, P. G., Coggan, M., Chelvanayagam, G., Easteal, S., Jermiin, L. S., Schulte, G. K., Danley, D. E., Hoth, L. R., Griffor, M. C., Kamath, A. V., Rosner, M. H., Chrunyk, B. A., Perregaux, D. E., Gabel, C. A., Geoghegan, K. F., and Pandit, J. (2000) *J. Biol. Chem.* **275,** 24798–24806
9. Mannervik, B. (1986) *Chem. Scr.* **26,** 281–284
10. Litwach, G., Ketterer, B., and Arias, I. M. (1971) *Nature* **234,** 466–477
11. Adler, V., Yin, Z., Fuchs, S. Y., Benezra, M., Rosario, L., Tew, K. D., Pincus, M. R., Ardana, M., Henderson, C. J., Wolf, C. R., Davis, R. J., and Ronai, Z. (1999) *EMBO J.* **18,** 1321–1334
12. Kampranis, S. C., Damianova, R., Atallah, M., Toby, G., Kondi, G., Tsichlis, P. N., and Mahkris, A. M. (2000) *J. Biol. Chem.* **275,** 29207–29216
13. Dulhunty, A., Gage, P., Curtis, S., Chelvanayagam, G., and Board, P. (2001) *J. Biol. Chem.* **276,** 3319–3323
14. Dirr, H. W., Reinemer, P., and Huber, R. (1994) *Eur. J. Biochem.* **220,** 645–661
15. Wilce, M. C. J., and Parker, M. W. (1994) *Biochim. Biophys. Acta* **205,** 1–18
16. Rossjohn, J., McKinstry, W. J., Oakley, A. J., Verger, D., Flanagan, J., Chelvanayagam, G., Tan, K.-L., Board, P. G., and Parker M. W. (1998) *Structure* **6,** 309–322
17. Wilce, M. C. J., Board, P. G., Feil, S. C., and Parker, M. W. (1995) *EMBO J.* **14,** 2133–2143
18. Lo Bello, M., Nuccetelli, M., Caccuri, A. M., Stella, L., Parker, M. W., Rossjohn, J., McKinstry, W. J., Mozzi, A. F., Federici, G., Polizio, F., Pedersen, J. Z., and Ricci, G. (2001) *J. Biol. Chem.* **276,** 42138–42145
19. Ueno, T., and Yoshimura, T. (2000) *Jpn. J. Pharmacol.* **82,** 95–101
20. Mulsh, A., Mordvintcev, P., Vanin, A. F., and Busse, R. (1991) *FEBS Lett.* **294,** 252–256
21. Mulsch, A., Mordvintcev, P., Vanin, A. F., and Busse, R. (1993) *Biochem. Biophys. Res. Commun.* **196**, 1303–1308
22. Muller, B., Kleschyov, A. L., and Stoclet, J. C. (1996) *Br. J. Pharmacol.* **119,** 1281–1285
23. Vanin, A. F., Malenkova, I. V., and Serezhenkov, V. A. (1997) *Nitric Oxide* **1,** 191–203
24. Vanin, A. F. (1991) *FEBS Lett.* **289,** 1–3
25. Manukhina, E. B., Malyshev, I. Y., Malenyuk, E. B., Zenina, T. A., Pokidyshev, D. A., Mikojan, V. D., Kubrina, L. N., and Vanin, A. F. (1998) *Biull. Eksp. Biol. Med.* **125,** 30–33
26. Mulsh, A. (1994) *Arzneim. Forsch.* **44,** 408–411
27. Malyshev, I. Y., Malugin, A. V., Golubeva, L. Y., Zenina, T. A., Manukhina, E. B., Mikojan, V. D., and Vanin, A. F. (1996) *FEBS Lett.* **391,** 21–23
28. Malyshev, I. Y., Zenina, T. A., Golubeva, L. Y., Saltykova, V. A., Manukhina, E. B., Mikojan, V. D., Kubrina, L. N., and Vanin, A. F. (1999) *Nitric Oxide* **3,** 105–113
29. Giannone, G., Takeda, K., and Kleyshov, A. L. (2000) *J. Physiol.* (*Lond.*) **529,** 735–745
30. Ricci, G., Lo Bello, M., Caccuri, A. M., Pastore, A., Nuccetelli, M., Parker, M. W., and Federici, G. (1995) *J. Biol. Chem.* **270,** 1243–1248
31. Lo Bello, M., Battistoni, A., Mazzetti, A. P., Board, P. G., Muramatzu, M., Federici, G., and Ricci, G. (1995) *J. Biol. Chem.* **270,** 1249–1253
32. Caccuri, A. M., Antonini, G., Ascenzi, P., Nicotra, M., Nuccetelli, M., Mazzetti, A. P., Federici, G., Lo Bello, M., and Ricci, G. (1999) *J. Biol. Chem.* **274,** 19276–19280

Downloaded from http://www.jbc.org/ by guest on July 18, 2018

33. Board, P. G., and Pierce, K. (1987) *Biochem. J.* **248,** 937–941
34. Ross, V. L., and Board, P. G. (1993) *Biochem. J.* **294,** 373–380
35. Tan, K.-L., Chelvanayagam, G., Parker, M. W., and Board, P. G. (1996) *Biochem. J.* **319,** 315–321
36. Flanagan, J. U., Rossjohn, J., Parker, M. W., Board, P. G., and Chelvanajagam, G. (1999) *Protein Sci.* **8,** 2205–2212
37. Perito, B., Allocati, N., Casalone, E., Masulli, M., Dragani, B., Polsinelli, M., Aceto, A., and DI Ilio, C. (1996) *Biochem. J.* **318,** 157–162
38. Gillham, B. (1971) *Biochem. J.* **121,** 667–672
39. Mendes, P. (1993) *Comput. Appl. Biosci.* **9,** 563–571
40. Mendes, P. (1997) *Trends Biochem. Sci.* **22,** 361–363
41. Mendes, P., and Kell, D. B. (1998) *Bioinformatics* **14,** 869–883
42. Caccuri, A. M., Antonini, G., Board, P. G., Parker, M. W., Nicotra, M., Lo Bello, M., Federici, G., and Ricci, G. (1999) *Biochem. J.* **344,** 419–425
43. Caccuri, A. M., Antonini, G., Board, P. G., Flanagan, J., Parker, M. W., Paolesse, R., Turella, P., Federici, G., Lo Bello, M., and Ricci, G. (2001) *J. Biol. Chem.* **276,** 5427–5431
44. Pedersen, J. Z., and Cox, R. P. (1988) *J. Magn. Reson.* **77,** 369–371
45. Dauber-Osguthorpe, P., Roberts, V. A., Osguthorpe, D., Wolff, J., Genest, M., and Hagler, A. T. (1988) *Proteins* **4,** 31–47
46. Koradi, R., Billeter, M., and Wuthrich, K. (1996) *J. Mol. Graphics* **14,** 51–55
47. Caccuri, A. M., Antonini, G., Board, P. G., Flanagan, J., Parker, M. W., Paolesse, R., Turella, P., Chelvanayagam, G., and Ricci, G. (2001) *J. Biol. Chem.* **276,** 5432–5437
48. Turella, P., Pedersen, J. Z., Caccuri, A. M., De Maria, F., Mastroberardino, P., Lo Bello, M., Federici, G., and Ricci, G. (2003) *J. Biol. Chem.* **278,** 42294–42299
49. McDonald, C. C., Phillips, W., and Mower, H. F. (1965) *J. Am. Chem. Soc.* **87,** 3319–3326
50. Mannervik, B., and Danielson, U. H. (1988) *CRC Crit. Rev. Biochem.* **23,** 283–336
51. Casalone, E., Allocati, N., Ceccarelli, I., Masulli, M., Rossjohn, J., Parker, M. W., and Di Ilio, C. (1998) *FEBS Lett.* **423,** 122–124
52. Caccuri, A. M., Antonini, G., Allocati, N., Di Ilio, C., De Maria, F., Innocenti, F., Parker, M. W., Masulli, M., Lo Bello, M., Turella, P., Federici, G., and Ricci, G. (2002) *J. Biol. Chem.* **277,** 18777–18784
53. Caccuri, A. M., Antonini, G., Allocati, N., Di Ilio, C., Innocenti, F., De Maria, F., Parker, M. W., Masulli, M., Polizio, F., Federici, G., and Ricci, G. (2002) *Biochemistry* **41,** 4686–4693
54. Boese, M., Mordvintcev, P. I., Vanin, A. F., Busse, R., and Mulsch, A. (1995) *J. Biol. Chem.* **270,** 29244–29249

Downloaded from http://www.jbc.org/ by guest on July 18, 2018

The Specific Interaction of Dinitrosyl-Diglutathionyl-Iron Complex, a Natural NO Carrier, with the Glutathione Transferase Superfamily: SUGGESTION FOR AN EVOLUTIONARY PRESSURE IN THE DIRECTION OF THE STORAGE OF NITRIC OXIDE

Francesca De Maria, Jens Z. Pedersen, Anna Maria Caccuri, Giovanni Antonini, Paola Turella, Lorenzo Stella, Mario Lo Bello, Giorgio Federici and Giorgio Ricci

J. Biol. Chem. 2003, 278:42283-42293.
doi: 10.1074/jbc.M305568200 originally published online July 18, 2003

Access the most updated version of this article at doi: 10.1074/jbc.M305568200

Alerts:
- When this article is cited
- When a correction for this article is posted

Click here to choose from all of JBC's e-mail alerts

This article cites 54 references, 24 of which can be accessed free at
http://www.jbc.org/content/278/43/42283.full.html#ref-list-1

Downloaded from http://www.jbc.org/ by guest on July 18, 2018